

Phase Dynamics Criterion for Fast Relaxation of High-Confinement-Mode Plasmas

P. W. Xi,^{1,2,*} X. Q. Xu,² and P. H. Diamond^{3,4}

¹*FSC and State Key Lab of Nuclear Physics and Technology, Department of Physics, Peking University, Beijing 100871, People's Republic of China*

²*Lawrence Livermore National Laboratory, Livermore, California 94550, USA*

³*WCI Center for Fusion Theory, National Fusion Research Institute, Daejeon 100871, Republic of Korea*

⁴*CASS and Department of Physics, University of California San Diego, La Jolla, California 92093-0429, USA*

(Received 28 August 2013; published 26 February 2014)

We derive a new nonlinear criterion for the occurrence of fast relaxation (crash) events at the edge of high-confinement-mode plasmas. These fast relaxation events called ELMs (edge-localized modes) evolve from ideal magnetohydrodynamics (MHD) instabilities, but the crash is not due only to linear physics. We show that for an ELM crash to occur, the coherence time of the relative phase between potential and pressure perturbations must be long enough to allow growth to large amplitude. This phase coherence time is determined by both linear and nonlinear dynamics. An ELM crash requires that the instability growth rate exceed a critical value, i.e., $\gamma > \gamma_c$, where γ_c is set by $1/\tau_c$ and τ_c is the phase coherence time. For $0 < \gamma < \gamma_c$, MHD turbulence develops and drives enhanced turbulent transport. The results indicate that the shape of the growth rate spectrum $\gamma(n)$ is important to whether the result is a crash or turbulence. We demonstrate that ELMs can be mitigated by reducing the phase coherence time without changing linear instability. These findings also offer an explanation of the occurrence of ELM-free H-mode regimes.

DOI: [10.1103/PhysRevLett.112.085001](https://doi.org/10.1103/PhysRevLett.112.085001)

PACS numbers: 52.35.Ra, 52.55.Fa, 52.55.Tn, 52.65.Kj

Impulsive, abrupt relaxation phenomena are ubiquitous in physics. Examples include, but are not limited to, the catastrophic breaking of elastic structures under stress [1], solar flare eruptions [2], fast magnetic reconnection and relaxation in astrophysical and laboratory plasmas, and edge-localized modes (ELMs) [3], which occur at the edge of high-confinement-regime (H-mode) [4] tokamaks. Bursty relaxation is of interest for many reasons but almost always because of the strong, rapid energy release which results. While the criticality conditions for relaxation often involve linear stability criteria, it is also often the case that the ultimate, dynamical mechanisms for relaxation are nonlinear. A persistent general question is what is the nonlinear criticality condition which actually determines when bursty relaxation occurs?

In this Letter, we answer the above question for ELM crashes in tokamaks. ELMs are fast relaxation phenomena which occur in the steep gradient edge region of H-mode plasmas. ELM crashes cause large transient heat loads on plasma facing components and remain an urgent issue for present and future fusion reactors like ITER. The correct understanding of ELM dynamics and an accurate criterion for predicting the onset of ELMs are of great interest to the fusion community. It is widely accepted that ELMs are driven by steep edge pressure and current gradients and triggered by robust, ideal magnetohydrodynamics (MHD) peeling-ballooning (P-B) instabilities [5,6]. However, in this Letter, we demonstrate that the onset of ELMs is governed by a novel nonlinear criterion $\gamma > \gamma_c$ rather than the linear criterion $\gamma > 0$. Our analysis is centered on the

dynamics of the relative phase between pressure and potential perturbations. Phase dynamics has been extensively studied in the context of pattern formation [7], and now it is shown to be important to the linear-nonlinear transition, the onset of ELM crashes, and the formation of filamentary structure. Our results propose an explanation for the existence of an ELM-free H mode and also suggest new ELM control methods to experimentalists.

This analysis is conducted using the same reduced MHD model from the study of Ref. [6] with additional gyroviscous terms [8] by using BOUT++ [9]. Boundary conditions for vorticity ϖ , pressure \bar{P} , and parallel vector potential A_{\parallel} are Dirichlet, Neumann, and zero Laplacian, respectively. No additional sources or sinks are in simulations for ELM crashing dynamics on the order of a few hundred Alfvén time scale. Resistivity, hyper-resistivity, and parallel ion viscosity are chosen to be $S = \mu_0 R_0 v_A / \eta = 2 \times 10^{10}$, $S_H = \mu_0 R_0^3 v_A / \eta_H = 2 \times 10^{14}$, and $\mu_{i\parallel} = 0.1 \omega_A R^2$ for typical pedestal plasmas [10]. The shifted circular equilibrium is based on JET (the second equilibrium described in Ref. [10]) and has minor radius $a = 1.22$ m, major radius $R_0 = 3.53$ m, and toroidal magnetic field $B_t = 1.99$ T. The normalized pressure gradient is $\alpha = -2\mu_0 q^2 R_0 P'_0 / B^2 = 2.17$ and magnetic shear is $s = r q' / q = 3.81$ at the peak pressure gradient location. The number of grid cells in each direction is $n_{\psi} = 516$, $n_{\theta} = 128$, and $n_{\zeta} = 129$, where ψ , θ , and ζ are the radial, poloidal, and toroidal coordinates, respectively. This equilibrium is linearly unstable to peeling-ballooning modes, and the most unstable mode has toroidal mode number $n = 20$, with normalized linear

growth rate $\gamma/\omega_A = 0.034$ for a constant density $n_0 = 10^{19} \text{ m}^{-3}$. According to the conventional model based upon purely linear peeling-ballooning theory [5], this equilibrium will have an ELM crash because it is unstable to P-B modes (see the Supplemental Material [11] for more information).

We start with a comparison between a single-mode simulation (SMS) and a multiple-mode simulation (MMS), where SMS and MMS are defined by different initial perturbations, as follows:

$$\tilde{f}_{t=0} = f_0 G_1(\psi) G_2(\theta) \cos n\zeta, \text{ SMS}, \quad (1)$$

$$\tilde{f}_{t=0} = f_0 G_1(\psi) G_2(\theta) \sum_{n=0}^{160} A_n \cos(n\zeta + \varphi), \text{ MMS}. \quad (2)$$

Considering the localized nature of peeling-ballooning modes, G_1 and G_2 are set to be Gaussian functions. In both cases, the initial perturbation has an amplitude of $\delta p/p_0 = 10^{-4}$ set by f_0 . In SMS, the initial perturbation has toroidal mode number $n = 20$, which is the most unstable mode. In MMS, the initial perturbation is a toroidal spectrum with random phase and amplitude.

In SMS, the pressure profile crashes at $t = 140\tau_A$ and relaxes further at $t = 300\tau_A$ [Fig. 1(a)]. Here, $\tau_A = 3.5 \times 10^{-7} \text{ s}$ is the Alfvén time. When pedestal crash occurs, filaments are generated [Fig. 1(b)] and evolve into fully developed turbulence [Fig. 1(c)]. Here the definition of a filament is a helical coherent structure which moves and bursts radially outward. In MMS, the pressure profile remains nearly unchanged during the whole simulation period [Fig. 1(d)]. There, the fluctuations do not generate filaments but evolve directly to the turbulent state, as shown in Figs. 1(e) and 1(f). Also, the fluctuations in MMS have a much narrower radial extent, as compared to those in SMS.

Figure 2(a) shows the time evolution of the ELM size, which measures the energy loss during the ELM crash and is defined as $\Delta_{\text{ELM}}(t) = \int_{\psi_{\text{in}}}^{\psi_{\text{out}}} d\psi \oint J d\theta d\zeta (P_0 - \langle P(t) \rangle_\zeta) / \int d\psi \oint J d\theta d\zeta P_0$. Here, ψ_{in} is the inner boundary of the

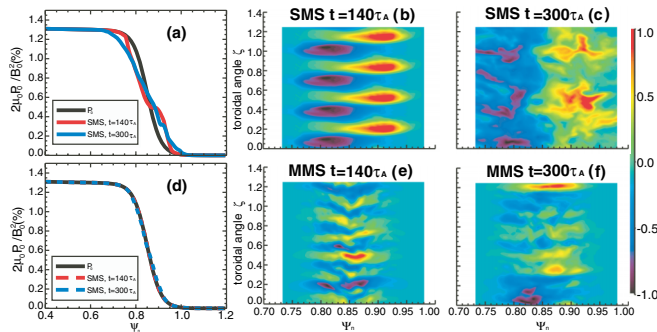


FIG. 1 (color online). Evolution of pressure profiles at different times is shown in (a) for SMS and (d) for MMS. The pressure fluctuation pattern at the outer midplane is shown in (b),(c) for SMS and (e),(f) for MMS. The toroidal segment is 4.

simulation domain, and ψ_{out} is chosen to be the location of the peak pressure gradient. P_0 is equilibrium pressure and J is Jacobian. In SMS, a typical ELM crash occurs at $t = 115\tau_A$, as indicated by the sudden increase in ELM size. This is consistent with linear theory. However, in MMS an ELM crash does not appear. Instead, slow turbulent transport occurs. Since the turbulence is generated by peeling-ballooning modes, it is named P-B turbulence. The energy loss for MMS is dramatically reduced relative to that for SMS. Clearly, MMS results disagree with the linear P-B model of the origin of ELM crashes.

These results show that the existence of linear instability alone does not predict ELM crashes. To trigger an ELM crash, the P-B perturbation must grow to a large, nonlinear amplitude. Linear drive and nonlinear wave-wave interaction both contribute to the growth of a mode. The linear drive in this model is mainly the ballooning drive, and it requires both sufficient growth rate and growth time to drive the mode. According to Eq. (1) of Ref. [6], the relation between the kinetic energy $\tilde{V}_{E \times B, n}^2$ and ballooning drive can be expressed as

$$\frac{\partial \tilde{V}_{E \times B, n}^2}{\partial t} \propto -2\Re(\text{in} \hat{\phi}_n^* \hat{P}_n \mathbf{b}_0 \times \kappa \cdot \nabla \zeta) \propto \sin \delta\varphi. \quad (3)$$

Here, the relative phase between \hat{P}_n and $\hat{\phi}_n$ is defined as $\delta\varphi(n, \psi, \theta, t) = \arg[\hat{P}_n(\psi, \theta, t) / \hat{\phi}_n(\psi, \theta, t)]$, $\delta\varphi \in (-\pi, \pi]$, where \hat{P}_n and $\hat{\phi}_n$ are the n th toroidal Fourier components of the pressure and potential perturbation, respectively. The relative phase is important because it determines whether

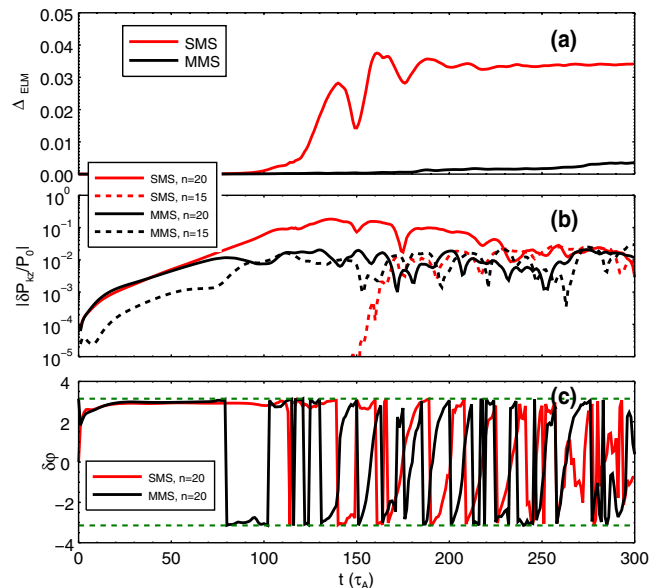


FIG. 2 (color online). Simulation results for SMS (red) and MMS (black). (a) Time evolution of ELM size; (b) time evolution of the toroidal Fourier component of pressure perturbation δP_{kz} ; (c) evolution of relative phase $\delta\varphi$ between \hat{P}_n and $\hat{\phi}_n$. The dashed green lines correspond to $\delta\varphi = \pm\pi$.

the ballooning mode can extract free energy from the pressure gradient or not. The curvature term drives ballooning modes when $0 < \delta\varphi < \pi$ (phase for growth) and damps ballooning mode when $-\pi < \delta\varphi < 0$ (phase for damping). Thus, the net increase in amplitude due to linear drive is set by $\gamma(n)\tau_c(n)$, where the phase coherence time (PCT) $\tau_c(n)$ is defined as the time duration of the phase for growth and is limited by nonlinear mode interaction.

In SMS, as shown in Figs. 2(b) and 2(c), there is no disruption in $\delta\varphi$ from wave-wave interaction prior to the ELM crash. The mode has a long time during which to grow to large amplitude and, thus, trigger an ELM crash. However, in MMS, wave-wave interaction starts at the beginning of the simulation. It scatters $\delta\varphi$ and terminates growth before the mode reaches a large amplitude. Consequently, the ELM crash is replaced by a quasistationary state of P-B turbulence. In the later turbulent state of both cases, $\delta\varphi$ fluctuates rapidly between positive and negative values; thus, τ_c becomes so short that no dramatic mode growth occurs. In addition, the strong consistency between phase coherence and the amplitude growth in Fig. 2 and Figs. 3(d) and 3(e) shows that the energy transfer among different modes via wave-wave interaction is much weaker than the linear drive in this model. In general, the scattering of $\delta\varphi$ naturally induces phase fluctuations and, thus, generates a statistical ensemble of phases. Here, τ_c is a stochastic quantity with a certain probability distribution function (PDF). The accurate measurement of this PDF requires an ensemble average over a huge database, and, thus, is beyond the scope of this Letter.

Overall, linear theory ignores the constraint set by τ_c and so leads to an underestimate of the critical growth rate for the onset of ELMs. The linear criterion $\gamma > 0$ for the onset of ELMs is, thus, seen as a necessary but not sufficient condition.

To find the sufficient condition for the onset of an ELM crash, we take the turbulent state of MMS at $t = 200\tau_A$ as the initial perturbation and examine the evolution of the pedestal pressure profile by scanning a range of equilibrium pressure gradients with other profiles fixed. Here we assume that the transport from the P-B turbulence is weaker than the heat flux from the core, so the pedestal gradient steepens until a crash is triggered. When the pressure gradient increases, the linear growth rates increases, as shown in Fig. 4(a). The evolution of fluctuations can be quite different, depending upon the product $\gamma(n)\tau_c(n)$. Three relevant possibilities are (a) P-B turbulence $\gamma(n)\tau_c(n) < \ln 10$, for all n ; (b) isolated crash $\gamma(n)\tau_c(n) > \ln 10$, for $n = n_d$ and $\gamma(n)\tau_c(n) < \ln 10$, for $n \neq n_d$; (c) turbulent crash $\gamma(n)\tau_c(n) > \ln 10$, for multiple n . The value $\ln 10$ is used to measure whether the mode amplitude can grow by an order of magnitude. Transport from P-B turbulence can be enhanced by the higher pressure gradient and may eventually balance the heat flux from the core. In this situation, an ELM-free H mode is obtained with a turbulent pedestal. Thus, our results

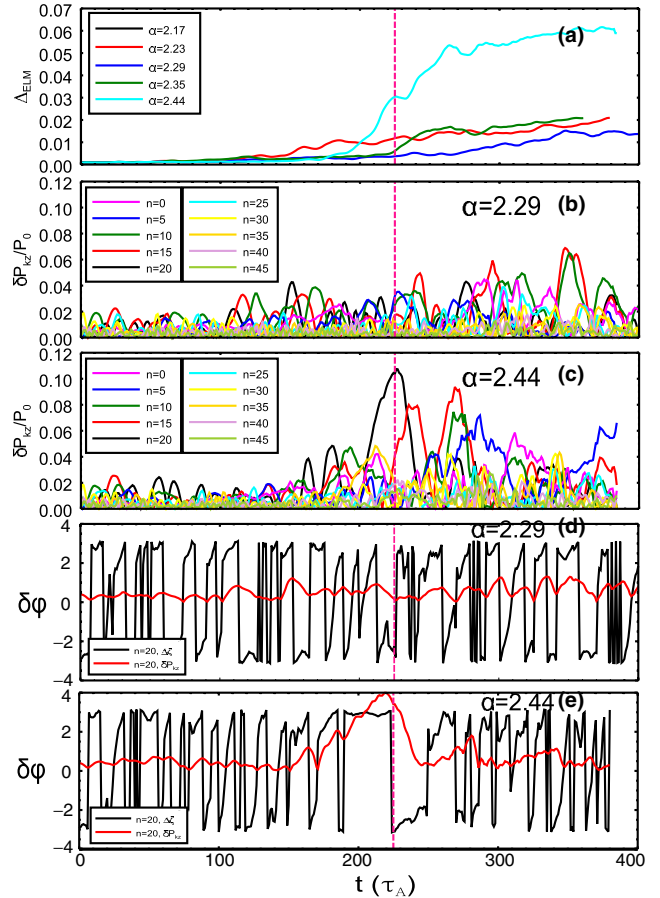


FIG. 3 (color online). (a) Time trace of ELM sizes for different pressure profiles. Fluctuation of different toroidal modes from $\alpha = 2.29$ case (b) and $\alpha = 2.44$ case (c). Time evolution of relative phase (black) and pressure perturbation (red) of $n = 20$ mode for $\alpha = 2.29$ case (d) and $\alpha = 2.44$ case (e).

suggest a possible explanation for the origin of ELM-free H mode. In the situation of an isolated crash, the mode with number n_d is called the dominant mode, because this mode grows to a large amplitude and triggers the crash. The dominant instability is determined by both $\gamma(n)$ and $\tau_c(n)$, and, thus, is not simply the most linearly unstable mode. If several modes can develop a long PCT at the same time and grow together, we can also observe a large “turbulent” crash, in which the ejected filament is composed of a mixture of different modes. Our analysis shows that ELM crashes not only depend on the magnitude of linear growth rates but also on the growth rate spectrum $\gamma(n)$. A peaked $\gamma(n)$ curve tends to trigger an isolated crash, while a flat $\gamma(n)$ curve leads to either P-B turbulence or a turbulent crash. This implies that in experiments, an isolated crash can be avoided by flattening the $\gamma(n)$ curve instead of by fully stabilizing all P-B modes.

In Fig. 3(a), only in the case with $\alpha = 2.44$ is an ELM crash triggered at $t = 200\tau_A$ by the dominant mode $n = 20$ [Fig. 3(c)]. In this case, the phase for growth persists for a long time—over $30\tau_A$ [Fig. 3(e)]. In cases with $\alpha < 2.44$,

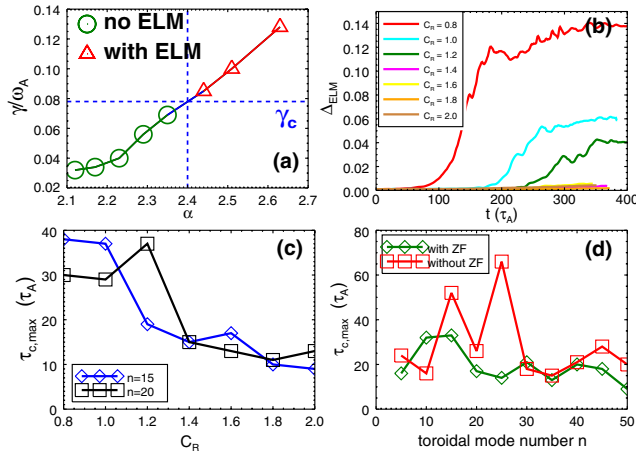


FIG. 4 (color online). (a) Maximum linear growth rates versus different α ; (b) time evolution of ELM size for different C_R values with $\alpha = 2.44$; (c) maximum τ_c versus C_R for $n = 15$ (blue) and $n = 20$ (black); (d) maximum τ_c for different mode numbers with $\alpha = 2.29$ for the case with (green) and without (red) zonal flow.

P-B turbulence leads to relatively slow transport. In those cases, no dominant mode appears, but all modes have similar amplitude, as shown in Fig. 3(b). This is due to the short τ_c [Fig. 3(d)]. In the case of P-B turbulence, the condition $\gamma\tau_c < \ln 10$ is satisfied. For the case of an ELM crash, the condition $\gamma\tau_c > \ln 10$ is satisfied by the dominant mode $n = 20$.

Overall, the sufficient condition for the onset of an ELM crash is $\gamma\tau_c > \ln 10$. This condition is equivalent to a constraint on the linear growth rate $\gamma > \gamma_c$, where $\gamma_c \sim \ln 10/\tau_c$ is the critical growth rate. In this work, $\gamma_c/\omega_A \sim 0.078$, as shown in Fig. 4(a). Unlike the purely linear criterion $\gamma > 0$, our novel criterion is nonlinear, since τ_c depends on the process of phase scattering.

Here we briefly sketch the derivation of the PCT and the phase diffusivity which determines it. Proceeding in the spirit of calculations of propagation in a random medium [12], we write $\hat{V}_r = B$, $\hat{P} = Ae^{i\delta\varphi}$, where A , B , and $\delta\varphi$ are real. $\delta\varphi$ is the relative phase between \hat{V}_r , and \hat{P} and is equivalent to what is commonly referred to as the ‘‘cross phase.’’ Here the ‘‘random medium’’ is the ensemble of P-B turbulence. Thus, the pressure response evolves according to $\partial\hat{P}/\partial t + \tilde{\mathbf{V}} \cdot \nabla\hat{P} - D_0\nabla^2\hat{P} = -\tilde{V}_r\partial\langle P \rangle/\partial r$, where ambient background diffusion D_0 allows nontrivial phase-amplitude coupling. For $D_0 = 0$, the phase evolution reduces to a simple scalar turbulence problem. Writing $\delta\varphi = \delta\varphi(\mathbf{x}, t)$, the phase evolution equation can straightforwardly be renormalized using standard methods [13,14], and we get the phase evolution equation

$$\frac{\partial\delta\varphi_{\mathbf{k}}}{\partial t} + \mathbf{k} \cdot \overleftrightarrow{D} \cdot \mathbf{k}\delta\varphi_{\mathbf{k}} = 0. \quad (4)$$

The phase diffusion tensor $\overleftrightarrow{D} = \sum_{\mathbf{k}'} \tilde{\mathbf{V}}_{\mathbf{k}'} L_{\mathbf{k}+\mathbf{k}'} \tilde{\mathbf{V}}_{\mathbf{k}'}$, where $L_{\mathbf{k}+\mathbf{k}'} = (\partial_t + 1/\tau_{c,\mathbf{k}+\mathbf{k}'})^{-1}$ is the propagator describes the

rate at which the P-B mode relative phase is scattered by stochastic advection by the velocities of other background P-B modes. Note that $D \sim (\tilde{V}^2/k^2)^{1/2}$. Here, $\mathbf{k} \cdot \overleftrightarrow{D} \cdot \mathbf{k}$, or, ignoring anisotropy, $k^2 D_{\delta\varphi}$ sets the time rate of change $\delta\varphi$, and, thus, can be used as a statistical approximation to the stochastic quantity τ_c^{-1} . The condition for a P-B crash due to mode n is then $\gamma(n) > \ln 10(k^2 D_{\delta\varphi})_n$. Note that this criterion is explicitly nonlinear via the amplitude dependence of $D_{\delta\varphi}$. The importance of the distribution of $\gamma(n)$ is also apparent. Without a dominant mode, a single filament crash could not occur. Finally, it is apparent that adding flow shear will enhance $1/\tau_c$ by the process of hybrid shear decorrelation [15].

According to our nonlinear criterion, ELMs can be controlled by decreasing τ_c without changing the linear drive. To show this, we place an artificial coefficient C_R in front of the nonlinear convection term in the vorticity equation, i.e., $\partial\varpi/\partial t + C_R \tilde{\mathbf{V}}_E \cdot \nabla\varpi = \text{RHS}$. By changing C_R , nonlinear mode interaction is modified, but linear instability is not affected. For the case with $\alpha = 2.44$, different C_R values give different ELM evolution, as shown in Fig. 4(b). Compared with the original case of $C_R = 1.0$, decreasing C_R to 0.8 weakens the mode interaction and, thus, phase scattering. Thus, the most unstable mode can grow more easily and so lead to a larger ELM crash at an earlier time. Increasing C_R generates much stronger nonlinear coupling and phase scattering, so the ELM crash is smaller and is eventually suppressed. Consistent with this, Fig. 4(c) shows that increasing C_R leads to shorter τ_c . Note that the maximum linear growth rate for the $\alpha = 2.44$ case is 0.085, so the τ_c needed to trigger an ELM crash is about $\tau_c \sim \ln 10/0.085 \approx 27\tau_A$. The cases with PCT shorter than this time do not crash but manifest P-B turbulence.

Finally, a simple study on the effect of zonal flow on τ_c is performed [Fig. 4(d)]. Overall, zonal flow can reduce the τ_c for most modes. Given the analysis above, it is not surprising that mean or zonal flow shear can decrease $\tau_c(n)$, due to the fact that it leads to an enhanced, hybrid phase decorrelation processes, i.e., $k_{\perp}^2 D_{\delta\varphi} \rightarrow (k_{\theta}^2 \langle V_{\perp} \rangle^2 D_{\delta\varphi})^{1/3}$. The basic trend of flow shear is to reduce the incidence of ELM crashes. Thus, the strong edge shear flows can be expected to be beneficial for ELM mitigation. This suggests a possible explanation for the Quiescent H-mode (QH).

In conclusion, we presented a new, nonlinear criterion for the ELM crash. The occurrence of the crash depends on both the linear MHD growth rate $\gamma(n)$ and the phase coherence time $\tau_c(n)$. The criterion for the crash is $\gamma > \gamma_c \sim \ln 10/\tau_c$ rather than the purely linear criterion $\gamma > 0$. This theory suggests that ELMs can be controlled by changing the growth rate spectrum or by shortening the phase coherence time. The control of $\gamma(n)$ and $\tau_c(n)$ via flow shear, magnetic shear or other equilibrium quantities, the spatiotemporal evolution of relative phase, the probability distribution function of $\tau_c(n)$, and the effect of finite diffusion on phase evolution are four important issues to

study in the future. More generally, this study points toward the key role of relative phase evolution in controlling bursty relaxation.

This work was performed under the auspices of the U.S. DOE by LLNL under Contract No. DE-AC52-7NA27344 and is supported by the NSFC under Grants No. 10935004 and No. 11261140326, the PKU Program No. 2013GB112006, the WCI program of Korea, and the CMTFO sponsored by the U.S. DOE. The authors wish to thank X. G. Wang, P. Snyder, F. L. Waelbroeck, T. Y. Xia, and G. Dif-Pradalier for useful discussions.

*Corresponding author. pwxipku@gmail.com

- [1] N. S. Trahair, *Flexural-Torsional Buckling of Structures* (CRC Press, Boca Raton, 1993), Vol. 6.
- [2] S. Tsuneta, *Astrophys. J.* **456**, 840 (1996).
- [3] H. Zohm, *Plasma Phys. Controlled Fusion* **38**, 105 (1996).
- [4] F. Wagner, G. Fussmann, T. Grave, M. Keilhacker, M. Kornherr, K. Lackner, K. McCormick, E. Müller, A. Stäbler, G. Becker *et al.*, *Phys. Rev. Lett.* **53**, 1453 (1984).
- [5] P. Snyder, H. Wilson, J. Ferron, L. Lao, A. Leonard, T. Osborne, A. Turnbull, D. Mossessian, M. Murakami, and X. Xu, *Phys. Plasmas* **9**, 2037 (2002).
- [6] X. Q. Xu, B. Dudson, P. B. Snyder, M. V. Umansky, and H. Wilson, *Phys. Rev. Lett.* **105**, 175005 (2010).
- [7] Y. Kuramoto, *Prog. Theor. Phys.* **71**, 1182 (1984).
- [8] P. Xi, X. Xu, T. Xia, W. Nevins, and S. Kim, *Nucl. Fusion* **53**, 113020 (2013).
- [9] B. Dudson, M. Umansky, X. Xu, P. Snyder, and H. Wilson, *Comput. Phys. Commun.* **180**, 1467 (2009).
- [10] X. Xu, B. Dudson, P. Snyder, M. Umansky, H. Wilson, and T. Casper, *Nucl. Fusion* **51**, 103040 (2011).
- [11] See the Supplemental Material at <http://link.aps.org/supplemental/10.1103/PhysRevLett.112.085001> for additional information on the simulations.
- [12] A. Ishimaru, *Wave Propagation and Scattering in Random Media* (Academic Press, New York, 1978), Vol. 2.
- [13] T. H. Dupree, *Phys. Fluids* **9**, 1773 (1966).
- [14] P. H. Diamond, S.-I. Itoh, and K. Itoh, *Modern Plasma Physics* (Cambridge University Press, Cambridge, England, 2010), Vol. 1.
- [15] H. Biglari, P. H. Diamond, and P. Terry, *Phys. Fluids B* **2**, 1 (1990).